Biogeosciences

EGU Open Access

Technical note: Continuous fluorescence-based monitoring of seawater pH in situ

John W. Runcie[1,2,3], **Christian Krause**[4], **Sergio A. Torres Gabarda**[1,3], **and Maria Byrne**[1,3]

[1]School of Life and Environmental Sciences, University of Sydney, Sydney, Australia
[2]Aquation Pty Ltd, Umina Beach, Australia
[3]Sydney Institute of Marine Sciences, Mosman, Australia
[4]Presens Precision Sensing GmbH, Regensburg, Germany

Correspondence: John W. Runcie (john.runcie@sydney.edu.au)

Abstract. Electrical conductivity (salinity), temperature and fluorescence-based measurements of pH were employed to examine diel fluctuations in seawater carbonate chemistry of surface waters in Sydney Harbour over two multiple-day periods. A proof-of-concept device employing the fluorescence-based technique provided a useful time series for pH. Alkalinity with pH and temperature were used to calculate the degree of calcite and aragonite saturation (Ω_{Ca} and Ω_{Ar}, respectively). Alkalinity was determined from a published alkalinity–salinity relationship. The fluctuations observed in pH over intervals of minutes to hours could be distinguished from background noise. While the stated phase angle resolution of the lifetime fluorometer translated into pH units was ± 0.0028 pH units, the repeatability standard deviation of calculated pH was 0.007 to 0.009. Diel variability in pH, Ω_{Ar} and Ω_{Ca} showed a clear pattern that appeared to correlate with both salinity and temperature. Drift due to photodegradation of the fluorophore was minimized by reducing exposure to ambient light. The Ω_{Ca} and Ω_{Ar} fluctuated on a daily cycle. The net result of changes in pH, salinity and temperature combined to influence seawater carbonate chemistry. The fluorescence-based pH monitoring technique is simple, provides good resolution and is unaffected by moving parts or leaching of solutions over time. The use of optics is pressure insensitive, making this approach to ocean acidification monitoring well suited to deepwater applications.

1 Introduction

Ocean carbon chemistry is predicted to vary in response to an elevated concentration of atmospheric carbon dioxide (CO_2), with a decline in pH and an increase in the partial pressure of dissolved CO_2 (pCO_2) over the coming decades. However, short-term diel changes in seawater pH and pCO_2 at the scale of an embayment are unlikely to represent predicted globally increasing trends. Seawater carbonate chemistry in shallow nearshore environments is more likely driven by a combination of biological (photosynthesis, respiration) and local hydrodynamic (tidal, low salinity surface- and/or ground-water input) processes (Santos et al., 2012) with typical variation at timescales ranging from minutes to days. Capturing these short-term fluctuations requires virtually continuous monitoring of water chemistry.

Seawater pH has been commonly measured with a potentiometric technique using glass electrodes. While this method can be accurate and precise if appropriate care is taken with temperature control and the use of seawater buffers (Dickson, 2010), this technology suffers from gradual drift that may be attributable to changes in the strain-induced asymmetry potential of the glass bulb and reference junction effects. In addition, common reference electrode designs are susceptible to poisoning, in particular by sulphide released when conditions become anoxic. However, recent advances in electrode design including the incorporation of double- (or even quadruple-) junction salt bridges have enabled the continuous use of glass pH electrodes in shallow marine waters for over 12 months (Ionode Pty Ltd, Australia, Matthew Newman, personal communication, 2015).

Spectroscopic techniques for measuring seawater pH use a pH-sensitive dye that assumes different absorbance spectra depending on pH. While the method can provide pH estimates with an uncertainty less than 0.01, variability in the purity of the dye obtained from commercial suppliers can cause the apparent extinction coefficients associated with a particular dye to differ slightly from published extinction coefficient values. Consequently, uncertainty associated with this technique is generally assumed to be about 0.015 pH units (Douglas and Byrne, 2017b).

Ion selective field effect transistor (ISFET) technology is becoming more widely used to measure pH in seawater. The pH sensors using ISFET technology comprise the ISFET sensor itself – a solid-state device with a H^+ ion-sensitive material, a counter electrode and a reference electrode. In pH monitoring systems such as the SeaFET (Martz et al., 2010; Takeshita et al., 2015; Johnson et al., 2016), a chloride electrode is used as reference as chloride ion activity is relatively constant in deep water. However, this introduces problems in locations where chloride concentrations may rapidly fluctuate, such as some euryhaline estuarine environments.

Optical fluorescence-based approaches to pH sensing offer an alternative to glass electrodes, spectrophotometric techniques and ISFET sensors. Optical fluorescence-based methods do not require electrolyte solutions or gels which gradually lose ions, nor do they require reference electrodes and their accompanying susceptibility to varying environmental conditions. Optical methods are also impervious to high pressure. Only the housing for the device and the window through which the optical signal is passed must be pressure resistant. The use of fluorescence lifetime measurements provides the additional advantage of being insensitive to changes in fluorescence intensity. As the fluorophores used in this study are sensitive to changes in temperature and salinity, careful measurement of these parameters remains essential.

In this study we explore a new approach to logging pH in seawater in the setting of an ocean-water dominated estuarine environment. We incorporated a commercially available fluorescence-based pH sensing system (Presens GmbH) in a submersible continuous-monitoring device (Aquation Pty Ltd) to measure short-term changes in seawater pH in surface waters in Sydney Harbour over two multi-day intervals in austral autumn and summer. Electrical conductivity and temperature were also measured, and an approximation for alkalinity was derived from a salinity–alkalinity relationship reported for the Australasian region (Lenton et al., 2016). We acknowledge that the relationship between salinity and alkalinity is subject to terrestrial influence, and consequently our estimate of alkalinity remains an approximation. With these data we estimated changes in seawater carbonate chemistry during the deployments. The objectives of the study were (a) to characterize the fluorescence-based pH monitoring system in seawater in terms of stability and resolution, and (b) to characterize diel fluctuations of pH and aragonite/calcite saturation state in surface waters. The study focussed on natural

fluctuations in seawater pH and the capability of the fluorescence technique to observe these fluctuations. Determining the uncertainty in pH values obtained from the fluorescence device was not an objective, as precise and accurate pH determinations would require considerable resources that were not available at the time of study.

2 Methods

2.1 Study site and sampling arrangements

Real-time measurements were made of seawater in the Sydney Harbour estuary at the Sydney Institute of Marine Sciences (SIMS), Chowder Bay, NSW, Australia (33.839357° S, 151.254587° E; Fig. 1). Chowder Bay is a shallow (5 to 10 m) embayment located on the northern shore of Sydney Harbour some 3 km from the ocean. Tides in Sydney Harbour (depths typically ∼ 20 m) are semi-diurnal, with a maximum difference of 1.95 m at the estuary entrance. Tidal fluctuation during the deployment intervals is referenced to measurements made at nearby Fort Denison (Caldwell et al., 2015). Seawater chemistry was measured from ∼ 1 m below sea level at low tide below the SIMS pier at Chowder Bay.

Two field deployments were conducted. Firstly, water was collected ∼ 1 m below low tide and pumped 3–5 m up into a 2 L reservoir in an enclosed structure at the end of the pier. Water exited the reservoir through a narrow tube located below an overflow pipe at the upper part of the reservoir, passing through a clear polycarbonate tube for optical measurement (ex situ measurements, autumn, 8–19 April 2016). Fluorescence spots were attached to the inside of this tube and a plastic optical fibre was positioned perpendicular to the outside of the tube and directed to the spot. To avoid photobleaching, the system was covered in black plastic eliminating most light. Waste water was directed back into the harbour at least 5 m away from the intake location. This preliminary series of tests enabled us to make frequent measurements as the system could use a constant supply of mains power. The primary objective of the ex situ measurements was to assess the stability of the system.

In situ measurements were later made ∼ 1 m below low tide during 14–22 December 2016, with the self-contained instrument (Fig. 2) attached vertically to a post under the pier and the fluorescence spot facing downwards to minimize sunlight-induced photobleaching. In this arrangement, the plastic optical fibre within the clear polycarbonate cylindrical housing of the instrument was oriented perpendicular to the faceplate. To ensure that the spot could not peel off, a non-fluorescent mesh was held in place over the spot with a plastic ring. This arrangement ensured that the spot was fixed in position and water could easily reach the fluorophore and respond to ambient pH. A small hole was drilled partway into the inside of the faceplate to bring the fibre tip closer to the spot, which was affixed to the external surface of the
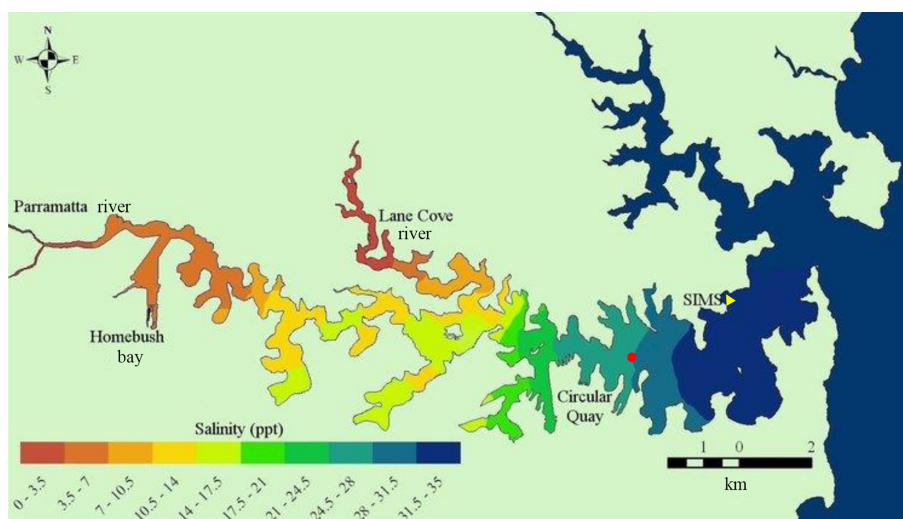
Figure 1. Port Jackson (Sydney Harbour) with sampling site (SIMS, yellow triangle) and Fort Denison tide reference station (red circle). The red dot on the map indicates Sydney's location. Map courtesy of Ian Jones and Daniel Harrison (http://www.sydneyharbourobservatory.org/projects-1/, last access: 6 July 2018).

Figure 2. Submersible logging pH monitor. The fluorescence spot is located on the upper faceplate between and forward of the two submersible connectors, beneath a clear plastic ring.

faceplate. This was necessary to increase signal strength to an acceptable level. During the in situ measurements, water samples were collected adjacent to the instrument and removed to the laboratory for measurement of pH_T (see below) within 30 min of sampling. The instrument contained

three nickel-metal hydride battery packs in series comprising 14 cells each with a total of 13.5 Ah at 16.8 volts.

Sunrise and sunset at the study site on 9 April 2016 were 06:14 and 17:38 AEST, respectively. Sunrise and sunset on 18 December 2016 were 05:40 and 20:02 AEST, respectively.

2.2 pH measurements

The fluorescence-based pH measurement uses a dual-luminophore frequency-domain fluorescence decay technique (Huber et al., 2001). A pH sensitive dye with short fluorescence decay time which changes its fluorescence intensity dramatically with pH is mixed together with an inert reference dye with long decay time. Both dyes are immobilized in particles which are dispersed in a hydrophilic membrane. This sensing membrane is in contact with the ambient water and a light guide is brought to the opposite site of the membrane to read the optical signal (Fig. 3). The read out unit (EOM-pH-mini) sends sine-wave-modulated blue light to excite both dyes simultaneously (the "spot") and measures the average decay time of the sum of returned fluorescence light from both dyes.

Calibration was performed prior to deployment of the instrument. All glassware, buffers, seawater and the instrument were left overnight in an air-conditioned room to reach a stable temperature of 22 °C. A pH cell with an Ag / AgCl reference electrode (Ionode Pty Ltd) was calibrated against standard buffers (pH 7.02 and 10.06 at 20 °C, Amalgamated Instruments Co. Pty Ltd, Australia). A pair of phosphate buffer solutions were also prepared, isotonic to ~ 34.5 ppt NaCl ($I = 0.7$ M) with B1 = 8.33 pH and B2 = 4.0 pH (where B1 and B2 are the measured pH of each of the buffers). A small
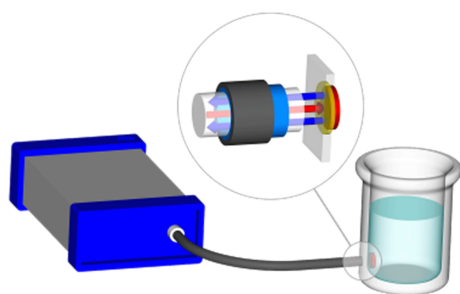
Figure 3. Schematic of pH monitoring system with EOM-pH-mini (left), and fibre optic conveying light to fluorescent spot attached to inside of vessel (right). The magnified circle shows light conveyed through the transparent vessel wall to the spot (red arrow), and fluorescent light emitted from the spot back along the fibre (blue arrows).

volume (e.g. 0.25 mL) of B1 was added to 10 mL of B2 until the combined buffer reached a pH of 4.45 as measured by the pH cell. An aliquot (approx. 1 mL) of this combined buffer solution of known pH was pipetted onto the fluorescence spot (fixed to the inside of the clear polycarbonate tube, or fixed to the faceplate of the instrument) and the fluorescence phase measured. Settling time of the phase value for each aliquot could take at least 10 min. Then, more B1 was added to the combined buffer and the process repeated at pH 5.66, 6.81, 7.23, 7.72, 8.02 and 8.30. The relationship between measured phase and (total) pH was determined with a non-linear Boltzmann sigmoid model using the software provided by the manufacturer. We report pH in the total hydrogen ion scale (as recommended by Dickson, 2010). Both room and buffer temperatures were stable during the calibration procedure at 22 and 22 ± 0.5 °C, respectively.

At the beginning and end of the in situ deployment, water samples were collected adjacent to the submerged pH monitor and transported to the nearby lab at SIMS. At each sampling time, three 200 mL glass jars were completely filled, and lids secured underwater to eliminate air bubbles. This process was repeated at least three times, with approximately 30 min between each sampling time. Within 30 min of collection, pH was measured spectrophotometrically with m-cresol purple indicator dye (Acros Organics, Lot # A0321770) using a custom-built automated system with a USB4000 fibre optic spectrophotometer (Ocean Optics) following SOP 6b (standard operating procedure) from Dickson et al. (2007) and calculations from Liu et al. (2011). Spectrophotometric measurements of pH_T were frequently validated using certified reference seawater (Dickson Standard Batch 145). The repeatability of the spectrophotometric technique in our laboratory is typically 0.006 at temperatures between 17 and 24 °C (standard deviation), with an accuracy very much dependent on the dye quality. We did not apply corrections for dye impurities, temperature and salinity variations as discussed in Douglas and Byrne (2017a, b) because obtaining

such highly accurate pH values was not an objective of this study. The uncertainty attributable to these combined factors is within approximately 0.015 (Douglas and Byrne, 2017b). The measured pH_T was corrected according to the calculated pH_T of the certified reference material using published values for total alkalinity (A_T), dissolved inorganic carbon (DIC) and salinity at the same temperature. This correction eliminates much of the variability due to dye quality, light source and cuvette scratches.

A subset of consecutive pH measurements over a 100 min period was sampled during each of the two deployments to determine the variability in measured pH as repeatability (standard deviation). The resolution attributable to the lifetime decay fluorometer (as stated by the manufacturer) can be matched with corresponding values of pH to provide resolution of pH measurement at the instrument level. Corrections for the in situ measurements were made against spectrophotometric measurements of the reference samples by calculating two average offsets between values of collected samples measured using the fluorometric device and the spectrophotometric device. One offset was derived for the beginning of the deployment and one for the end. The gradual decline in measured values over time was corrected assuming a constant linear drift.

In situ measurements were taken 10 times per minute and averaged over 1 min before analysis. Ex situ measurements were taken once per minute and a running average of 10 min of the ex situ measurements is presented.

2.3 Temperature

PT100 sensors (resistance thermometers) were either suspended in the 2 L reservoir that received seawater immediately prior to ex situ measurements or were simply positioned up against the inside of the housing wall when deployed in situ. Initial temperature data during the in situ deployment were ignored until the sensors reached equilibrium with ambient water. In situ measurements were taken 10 times per minute and averaged over 1 min before analysis. Ex situ measurements were taken twice per minute and a running average of 10 min is presented.

2.4 Salinity

Electrical conductivity was measured using a Hanna HI3001 four-ring potentiometric conductivity probe designed for flow-through sensing wired to a custom circuit board. Millivolt values were converted to salinity assuming a linear relationship between sensor readings and salt content. The sensor was calibrated directly against a pure NaCl solution across a range of concentrations (0 to 40 ppt) at temperatures similar to that expected for seawater at the sampling location (23 °C). Uncertainty due to differences in conductivity of a pure NaCl solution at 35 ppt and $S = 35$ was assumed to be small. In situ measurements were taken 10 times per minute and averaged

over 1 min before analysis. Ex situ measurements were taken 3 times per minute and a running average of 10 min of the ex situ measurements is presented.

2.5 Data logging and calculations

Both flow-through and in situ deployments were conducted using a custom data logger/controller system based on a submersible data logger (Aquation Pty Ltd, Australia). All data were saved on board and downloaded to PC after retrieval of the instrument. Alkalinity was calculated from salinity data according to a linear salinity–alkalinity relationship for Australasian waters described by Lenton et al. (2016). Drift and offset corrections were made to the raw data as required (described above), and final pH, salinity, temperature and alkalinity values were used (with equilibrium constants from Mehrbach et al., 1973 refit by Dickson and Millero, 1987) to calculate Ω_{Ca} and Ω_{Ar} in CO2Sys (V2.1) (Dickson and Millero, 1987). The final pH is reported on the total scale.

3 Results

3.1 pH

Seawater collected and pumped to the sensor varied by 0.08 pH units from 7.97 to 8.05 over the 3-day interval in autumn (Fig. 4). The phase angle resolution of the lifetime fluorometer was stated by the manufacturer as 0.05°, and this translated to an instrument resolution of 0.0028 pH units when calibrated against the phosphate buffer mixtures. The measurement technique is also constrained by the stated resolution of 0.01 pH units) of the fluorescence spots. The repeatability standard deviation of calculated pH_T (derived from 100 min of consecutive measurements during each deployment) was 0.009 and 0.007 pH units for the April and December deployments, respectively. The best precision can be achieved by averaging multiple measurements, although this will of course hide real variability. Gradual bleaching is known to influence fluorophores (Lakowicz, 2006), contributing to a steady drift. This was accounted for with corrections based on samples collected in situ as described above. In this case, the decline in pH was 0.0136 pH units per day which is approximately 3 times the drift associated with measurement-induced bleaching of 0.003 pH units per 1000 measuring points as stated by the manufacturer. The pH measured over summer ranged from 7.95 to almost 8.15 units, some 0.1 units more basic than autumn values (Fig. 5).

3.2 Temperature

Surface seawater temperature fluctuated between 21.6 and 22.6 °C in April (ex situ measurements, Fig. 4), and 21.0 to 23.6 in December (in situ measurements, Fig. 5). The stated resolution of the PT100 temperature sensors was 0.01 °C and

concurrent readings were within 0.05 °C of each other. Over the 3-day period, temperature showed a consistent pattern of declining at night and then rapidly increasing again around the middle of the day, reaching a maximum value around mid-afternoon. During the in situ deployment, diel fluctuations in ambient seawater temperature varied between 1 and 2 °C, and increased to 23.6 °C in the last 2 days of the measuring interval (Fig. 5).

3.3 Salinity

Salinity was calculated from electrical conductivity, and ranged from 33.0 to 34.3 ppt during the ex situ measurements, and 34.6 to 37.7 during the in situ measurements with a mean value of 36.5 ppt during the in situ measurements (Figs. 4 and 5, respectively). Diel variation tracked the tidal cycle with higher salinity driven by the incoming tide (Fig. 4). However, the amplitude of the salinity signal was not consistently coincident with the tidal amplitude (Fig. 5).

3.4 Saturation states

Both Ω_{Ca} and Ω_{Ar} calculated from water in the ex situ trial fluctuated over the course of 3 days, providing a smoothed approximation of diel variation in these two parameters (Fig. 6). Most striking is the noise associated with the calculated values, reaching Ω unit values as high as 1. As a consequence of the definition of saturation state and due to the higher solubility of aragonite, and from specific values of K_{sp} for aragonite and calcite, Ω_{Ar} was slightly less variable than Ω_{Ca} (with values between 2.5 and 3.1 for Ω_{Ar} and between 3.8 to 5.4 for Ω_{Ca}, Fig. 6).

4 Discussion

4.1 Instrumentation

The fluorescence-based pH measurements provide sufficient resolution to observe and predict diel changes in nearshore system pH and indicated significant changes in seawater/carbonate chemistry at timescales of hours to days. Values of pH, salinity and temperature were all within what one would expect for the harbour at that time of year (e.g. pH ~ 8.0, $S = \sim 35$ ppt, $T = \sim 18$ °C; John Runcie, personal observation, 2016). Further, the average magnitude of both Ω_{Ca} and Ω_{Ar} were within the bounds of expected values for current-day marine surface waters. While an attempt was made to minimize exposure of the sensor spot to ambient light, the rate of drift observed in the instrument due to photobleaching may have been greater during the day. Photobleaching-induced drift could be further reduced by excluding all ambient light and by reducing the sampling frequency. This would be needed for longer-term deployments. Calibration against high-accuracy pH measurements at least at the beginning and end of a deployment, and more fre-
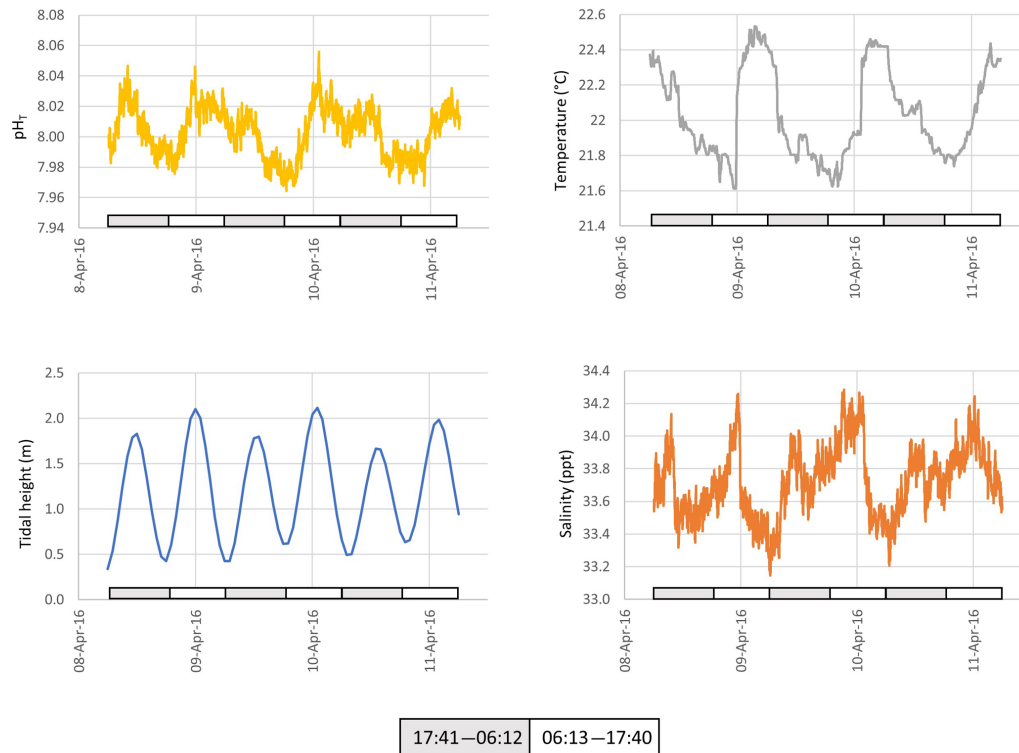
Figure 4. The pH, temperature, tidal height and salinity of seawater pumped from ∼ 1 m below low water at Chowder Bay, Sydney over a 3-day period. Grey and white boxes indicate the time between sunset and sunrise.
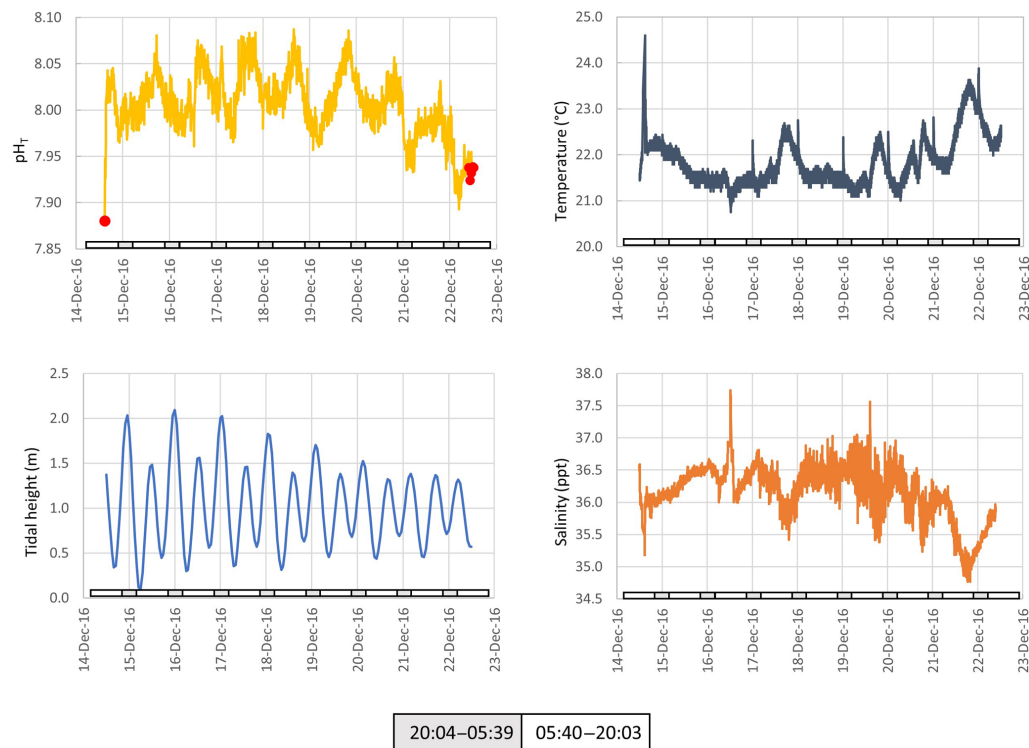

Figure 5. The pH, temperature, tidal height and salinity of seawater measured in situ at ∼ 1 m below low water at Chowder Bay, Sydney over a multi-day period. Grey and white boxes indicate the time between sunset and sunrise. Red dots indicate values of reference samples collected adjacent to the device and measured using spectrophotometry.
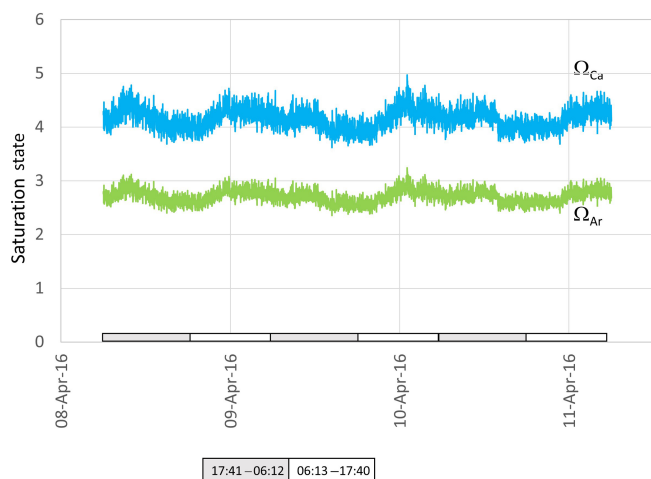
Figure 6. Aragonite (green) and calcite (blue) saturation values calculated from data presented in Fig. 4. Grey and white boxes indicate the time between sunset and sunrise.

Figure 7. Aragonite (green) and calcite (blue) saturation values calculated from data presented in Fig. 5. Grey and white boxes indicate the time between sunset and sunrise.

quently for an extended deployment, would be required to maintain suitably accurate data.

The mains-powered instrument designed to measure water pumped up from the harbour had the advantage of unlimited power and the capacity to make multiple measurements several times per minute. However, the dissolved gas content of pumped water can vary relative to the source water due to degassing and temperature changes, making measurements potentially less representative of the water to be sampled. We kept this to a minimum by pumping water over a short distance. Further, the need to use a suitable secure location with a constant power source is a limitation with respect to field deployments. In contrast, the battery-powered instrument tested during December 2016 had sufficient power to operate unattended for several weeks, and with a decrease in sampling frequency the lifetime of the unit could be extended to several months. For even longer periods, the device could be constructed with a longer cylinder containing extra battery packs or batteries could be replaced with lithium ion batteries. With this approach, the unit could be powered to operate unattended for over 12 months.

The housing used in this study was constructed from 5 mm thick acrylic. However, calculations indicate failure of the housing at depths exceeding 100 m. A metal housing with regular bulkheads along its length would increase pressure resistance and provide an instrument capable of withstanding deep ocean pressures, although a system with improved precision would be required for deep ocean work as the variation in pH at depth is low relative to surface waters.
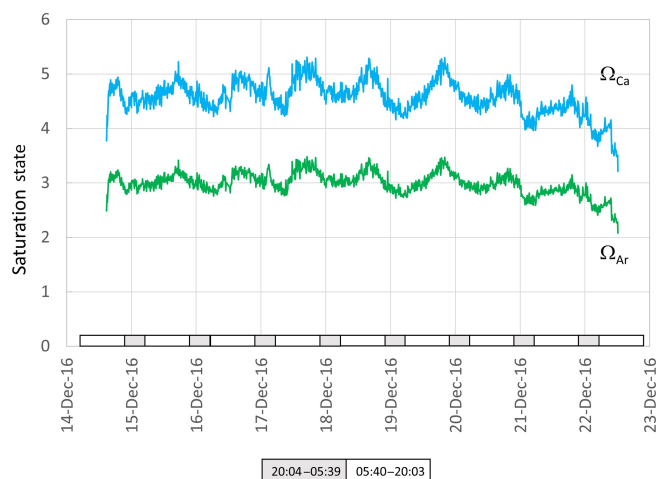
4.2   Data and significance

While there was a clear diel fluctuation in temperature of about 1 °C both in December and April, the gradual increase in temperature during the 20 and 21 December (austral summer) was coincident with a decline in salinity and tidal amplitude (Fig. 5). This suggests an influx of warmer freshwater into the estuary coupled with weaker tidal pumping, where pumping corresponds with flushing of the harbour with higher-salinity seawater from the ocean. The pH, Ω_{Ca} and Ω_{Ar} also declined during these last 2 days of the deployment (Fig. 7). These data show the important role that temperature and salinity play in determining seawater carbonate chemistry (Millero, 1995). Further, as the saturation state in this study is in part derived from alkalinity which is in turn derived from salinity and temperature, the importance of obtaining accurate measurements of temperature and salinity is to be emphasized. As a consequence of these physical factors (and presumably photosynthesis and respiration; Schulz and Riebesell, 2013), nearshore coastal waters and estuaries experience changes in Ω_{Ca} and Ω_{Ar} not only over the course of several days but also over a 24 h period. This contrasts with oceanic marine waters that maintain relatively constant values of saturation state. Models used to forecast seawater carbonate chemistry, such as those employed in the IPCC reports, are typically based on the open ocean. The projections for the open ocean do not incorporate the short-term fluctuations typical of coastal waters (Hendriks et al., 2015).

When assessing nearshore shallow-water marine coastal and estuarine environments, these short-term fluctuations in seawater carbonate chemistry can be significant, as found in this study, and are best accounted for and included in predictive models. Perhaps what is most important is to determine the capacity for organisms that live in these highly fluctuating

environments to withstand or thrive in spite of such a regular chemistry change. In this study we generated a targeted data set to assess the application of the fluorescence-based method for measuring seawater pH. Our results show the influence of fluctuating temperature and salinity on calcium carbonate saturation state in an estuarine environment. More research is needed to determine these and other drivers of fluctuating saturation states in detail (e.g. photosynthesis and respiration), and the actual consequences of these changes to key resident marine species.

4.3   Conclusion

We observed pH of surface water at Chowder Bay in Sydney Harbour to vary significantly across a diel cycle, influenced by temperature, salinity, tidal height, or alternating dominance of fresh or saline water. The fluorescence-based pH monitoring technique used here could resolve changes in pH to 0.007 pH units. Corresponding saturation states of calcite and aragonite (Ω_{Ca} and Ω_{Ar}) calculated from pH, temperature and salinity-derived alkalinity values showed diel fluctuations in seawater carbonate chemistry that can be interpreted as the combined effect of pH, temperature and salinity. Variability in saturation state over such short timescales in this shallow ecosystem indicates the importance of high temporal and spatial resolution measurements of seawater carbonate chemistry when determining the impact of ocean acidification on shallow nearshore marine and estuarine ecosystems.

References

Caldwell, P. C., Merrfield, M. A., and Thompson, P. R.: Sea level measured by tide gauges from global oceans – the Joint Archive for Sea Level holdings (NCEI Accession 0019568), Version 5.5, NOAA National Centers for Environmental Information, Dataset, https://doi.org/10.7289/V5V40S7W, 2015.

Dickson, A. G.: The carbon dioxide system in seawater: equilibrium chemistry and measurements, in Guide to best practises for ocean acidification research and data reporting, edited by: Riebesell, V. J., Fabry, V. J., Hansson, L., and Gattuso, J.-P., Publications Office of the European Union, Luxembourg, 17–40, 2010.

Dickson, A. G. and Millero, F. J.: A comparison of the equilibrium constants for the dissociation of carbonic acid in seawater media, Deep-Sea Res., 34, 1733–1743, https://doi.org/10.1016/0198-0149(87)90021-5, 1987.

Dickson, A. G., Sabine, C. L., and Christian, J. R.: Guide to best practices for ocean CO$_2$ measurements, PICES Special Publication, Sidney, Canada, 191 pp., 2007.

Douglas, N. K. and Byrne, R. H.: Achieving accurate spectrophotometric pH measurements using unpurified meta-cresol purple, Mar. Chem., 190, 66–72, https://doi.org/10.1016/j.marchem.2017.02.004, 2017a.

Douglas, N. K. and Byrne, R. H.: Spectrophotometric pH measurements from river to sea: Calibration of mCP for $0 \le S \le 40$ and $278.15 \le T \le 308.15$ K, Mar. Chem., 197, 64–69, https://doi.org/10.1016/j.marchem.2017.10.001, 2017b.

Hendriks, I. E., Duarte, C. M., Olsen, Y. S., Steckbauer, A., Ramajo, L., Moore, T. S., Trotter, J. A., and McCulloch, M.: Biological mechanisms supporting adaptation to ocean acidification in coastal ecosystems, Estuar. Coast. Shelf S., 152, A1–A8, https://doi.org/10.1016/j.ecss.2014.07.019, 2015.

Huber, C., Klimant, I., Krause, C., and Wolfbeis, O. S.: Dual Lifetime Referencing as Applied to an Optical Chloride Sensor, Anal. Chem., 73, 2097–2103, 2001.

Johnson, K. S., Jannasch, H. W., Coletti, L. J., Elrod. V. A., Martz, T. R., Takeshita, Y., Carlson, R. J., and Connery, J. G.: Deep-Sea DuraFET: A Pressure Tolerant pH Sensor Designed for Global Sensor Networks, Anal. Chem., 88, 3249–3256, https://doi.org/10.1021/acs.analchem.5b04653, 2016.

Lakowicz, J. R.: Principles of Fluorescence Spectroscopy, 3rd edn., Springer, New York, USA, 2006.

Lenton, A., Tilbrook, B., Matear, R. J., Sasse, T. P., and Nojiri, Y.: Historical reconstruction of ocean acidification in the Australian region, Biogeosciences, 13, 1753–1765, https://doi.org/10.5194/bg-13-1753-2016, 2016.

Liu, X., Patsavas, M. C., and Byrne, R. H.: Purification and characterization of meta-cresol purple for spectrophotometric seawater pH measurements, Environ. Sci. Technol., 45, 4862–4868, https://doi.org/10.1021/es200665d, 2011.

Martz, T. R., Connery, J. G., and Johnson, K. S.: Testing the Honeywell Durafet (R) for seawater pH applications, Limnol. Oceanogr.-Meth., 8, 172–184, https://doi.org/10.4319/lom.2010.8.172, 2010.

Mehrbach, C., Culberson, C. H, Hawley, J. E., and Pytkowicx, R. M.: Measurement of the apparent dissociation constants of carbonic acid in seawater at atmospheric pressure, Limnol. Oceanogr., 18, 897–907, 1973.

Millero, F. J.: Thermodynamics of the carbon dioxide system in the oceans, Geochim. Cosmochim. Ac., 59, 661–677, https://doi.org/10.1016/0016-7037(94)00354-O, 1995.

Runcie, J. and Byrne, M.: Sydney Harbour pH data 2016, The University of Sydney, https://doi.org/10.25910/5b42ef77e2991, 2018.

Santos, I. R., Eyre, B. D., and Huettel, M.: The driving forces of porewater and groundwater flow in permeable coastal sediments: A review, Estuar. Coast. Shelf S., 98, 1–15, https://doi.org/10.1016/j.ecss.2011.10.024, 2012.

Schulz, K. G. and Riebesell, U.: Diurnal changes in seawater carbonate chemistry speciation at increasing atmospheric carbon dioxide, Mar. Biol., 160, 1889–1899, https://doi.org/10.1007/s00227-012-1965-y, 2013.

Takeshita, Y., Frieder, C. A., Martz, T. R., Ballard, J. R., Feely, R. A., Kram, S., Nam, S., Navarro, M. O., Price, N. N., and Smith, J. E.: Including high-frequency variability in coastal ocean acidification projections, Biogeosciences, 12, 5853–5870, https://doi.org/10.5194/bg-12-5853-2015, 2015.